

Severity classification of ground-glass opacity via 2-D convolutional neural networks and lung CTs: a 3-day exploration

Lisa Y. W. Tang

Abstract

Ground-glass opacity is a hallmark of numerous lung diseases, including patients with COVID19 and pneumonia. This brief note presents experimental results of a proof-of-concept framework that got implemented and tested over three days as driven by the third challenge entitled "COVID-19 Competition", hosted at the AI-Enabled Medical Image Analysis Workshop of the 2023 IEEE International Conference on Acoustics, Speech and Signal Processing (ICASSP 2023). Using a newly built virtual environment (created on March 17, 2023), we investigated various pre-trained two-dimensional convolutional neural networks (CNN) such as Dense Neural Network, Residual Neural Networks, and Vision Transformers, as well as the extent of fine-tuning. Based on empirical experiments, we opted to fine-tune them using ADAM's optimization algorithm with a standard learning rate of 0.001 for all CNN architectures and apply early-stopping whenever the validation loss reached a plateau. For each trained CNN, the model state with the best validation accuracy achieved during training was stored and later reloaded for new classifications of unseen samples drawn from the validation set provided by the challenge organizers. According to the organizers, few of these 2D CNNs yielded performance comparable to the baseline developed by the organizers. As part of the challenge requirement, the source code produced during the course of this exercise is posted at <https://github.com/lisatwyw/cov19>. We also hope that other researchers may find this light prototype consisting of few Python files based on PyTorch 1.13.1 and TorchVision 0.14.1 approachable.

Keywords: Computed Tomography; pulmonary parenchymal involvement; ground-glass opacity severity; DenseNet; Residual Network; Inception; Wide Residual Network; VisionTransform; SqueezeNet; VGG; AlexNet

1 Introduction

Ground-glass opacity (GGO) is a hallmark of numerous lung diseases and typically signifies lung consolidation.

This manuscript documents the initial experimental work done on the open-source dataset named "COV19CT-DB" (COVID-19 Computed Tomography Database) as part of a challenge submission to the third competition entitled "ICASSP: COVID19 severity detection challenge".

Numerous studies [17, 19] from the past five years have shown the success of transfer learning of CNNs trained using three-channel two-dimensional inputs. Accordingly, we approach severity classification of GGO similarly. To this end, we explored the use of various CNNs architectures: AlexNet [12], VGG [15], Residual Networks [11], Vision Transformers [14] and DenseNet [18].

2 Materials

The training and validation samples is derived as a subset of a larger dataset named "COV19-CT-DB" that dataset contains over one thousand patient samples of three-Dimensional CT chest scans as archived in "lossy" image format (i.e. JPG). As further elaborated in previous articles [2, 1, 3, 4, 5, 6], these CT volumes were collected from different hospitals in the United States.

Due to time constraints (i.e. three days), this document focuses on the severity classification problem where each CT volume will be labeled as either "mild", "moderate", "severe", or "critical" [2]. These categories were predetermined by a pre-existing protocol where experts visually inspected each scan for lung disease morphology known as *groundglass opacity* (GGO) and manually labeled each as mild if none or fewer than 26% of the lungs were judged to capture "pulmonary parenchymal involvement" (see Figures 1-2 for examples); "moderate" if the involvement is 26-50%; "severe" if involvement is 50-70%; or "critical" if involvement is greater than 75% [16].

3 Methods

We propose the deployment of fine-tuned convolutional neural networks (CNNs) for the classification task. For ease of optimization, our approach explores a previous framework that leveraged two-dimensional Residual Networks [17] for the identification of a lung disease. The source code developed during the course of this experimental prototyping period is posted at <https://github.com/lisatwyw/cov19>.

3.1 Preprocessing

As the information on field of volume and voxel spacing is no longer accessible in the archival format provided in the challenge (i.e. JPG), the depth of the volume was approximated by the file counts n of each scan / folder.

The axial section centered at z was computed deterministically ($z = \lfloor n * .25 \rfloor$) based on parameters which were set based on visual inspection on a subset of the images randomly drawn from the training set. Then, three contiguous slices centered at z were concatenated to form three-channel inputs of size $3 \times b \times v$ where v depends on the CNN model [17].

Lung masks were next computed to retain only regions of the lungs (i.e. regions outside of the rib cage masked out). The implementation code of lung mask generation was adopted from online resource [21] such that the threshold parameter is adjusted so it will operate on the compressed data as stored in the JPG images from COV19-CT-DB, i.e.:

```
from skimage.segmentation import clear_border
init_roi_mask = jpeg_im_slice <100 # Updated
roi_mask_v0 = clear_border(init_roi_mask)
...
```

3.2 Model-training and selection

Each model architecture was fine-tuned over a maximum of 500 epochs. We used the categorical cross-entropy objective and optimization algorithm with a standard learning rate of 0.001 for all CNN architectures and applied early-stopping whenever the validation loss reached a plateau. Two optimization algorithms explored were Adams and Stochastic Gradient Descent (SGD). For SGD, the standard setting of using momentum value of 0.9 and weight decay of 0.0001 was used.

The following settings were tuned from a selection of choices: batch size $BS=\{16,128\}$, $LR=\{0.001,0.01\}$. Further, to enhance robustness against deformations and scale transformations, we explored the application of random horizontal flips and random rigid transformations, applied at 50% of the times (probability of 0.5).

For each trained CNN, the state with the best validation accuracy achieved during training was selected for the evaluation of each test sample.

3.3 Extent of fine-tuning

We initialized each CNN with pretrained weights and subsequently explored two level of network fine-tuning: allowing the network weights of all layers or only the last layer to be changed/optimized.

4 Results

This section is still being updated.

Table 1 and 2 report preliminary comparisons of the accuracies (F1-macro score) achieved by individual models as evaluated on the unseen validation set.

5 Conclusion

In this brief note, we shared empirical data that explored the feasibility of severity classification without the deployment of three-dimensional neural networks. We hope that other researchers may find this quick prototype consisting of few Python files based on PyTorch 1.13.1 and TorchVision 0.14.1 approachable.

Acknowledgements

The author sincerely thank Professor Dimitrios Kollias and the organizing committee for provisioning the COV19-CT-DB dataset and hosting this exciting challenge [2, 1, 3, 4, 5, 6]. The author would also like to express gratitude to Compute Canada/Alliance Canada as well as Tong Tsui Shan and Kim Chuen Tang for their in-kind support.

Model	Key settings		Overall F1		Class-wise F1		Pred. distr.
	FT	BS	Val	Unseen*	Val	Unseen*	
AlexNet [12]							
DenseNet [18]	last	512	56.5	62.2			110, 33, 86, 2
DenseNet201	last	16	63.2	67.9			105, 51, 73, 2
DenseNet201	last	512	57.2	64.3	100, 78.7, 72.6, 76.4	100, 87, 71.9, 77.6	91, 78, 51, 11
InceptionNet [9]	all	16					
InceptionNet [9]	last	16			100, 67.1, 49.7, 55.2	100, 67.6, 49.0, 56.4	
SqueezeNet [8]	all	16					231, 0, 0, 0
ResNet152 [11]	last	512	79.6	75.2			84, 102, 43, 2
ResNet152 [11]	last	64	54.0	53.6			110, 81, 40, 0
ResNet152 [11]	last	32	54.6	50.6			136, 64, 31, 0
ResNet152 [11]	all	16	100.0	100.0			
VGG [15]	last	16	92.6	91.6			198, 31, 2, 0
VGG [15]	last	512	94.0	94.9			176, 54, 1, 0
VTB32 [14]	last	16	71.9	68.7	100, 94.4, 78.2, 77.3		172, 0, 59, 0

Table 1: Comparative analysis of different fine-tuned CNNs under two key settings. Shown are the overall and class-wise F1-scores expressed in percentages. *Performance of CNNs when evaluated on unseen validation set. “FT” denotes the extent of fine-tuning: network weights from all layers or only the last layer were optimized. “Pred. distr.” denotes the predicted class distribution on the test set. **Please note that this table is still being updated.**

Model	Key settings		Overall F1		Class-wise F1		Pred. distr.
	$BS = 32$		Val	Unseen*	Val	Unseen*	
AlexNet			13.8	15.4			0, 0, 231, 0
DenseNet			59.7	61.7			104, 38, 89, 0
Inception			50.4	56.9	100, 74.2, 58.6, 60.9	100, 73.4, 62.6, 69.3	45, 35, 145, 6
DenseNet201			57.3	61.4	100, 81.9, 72.0, 72.0	100, 88.6, 62.1, 67.5	98, 59, 71, 3
ResNet152			54.6	50.6	100, 84.0, 79.2, 76.8	100, 73.5, 78.2, 75.4	136, 64, 31, 0
SqueezeNet			100	100			231, 0, 0, 0
VGG			94.0	91.8	100, 94.3, 91.2, 98.0	100, 96.5, 89.9, 97.0	194, 35, 2, 0
VTB32			73.0	70.2	100, 94.4, 78.2, 78.4	100, 96.5, 80.8, 84.0	202, 13, 13, 3
Wide ResNet101			82.8	85.9	100, 93.3, 87.3, 91.2	100, 94.3, 89.3, 94.0	153, 62, 16, 0

Table 2: Comparative analysis of different fine-tuned CNNs under another set of hyper-parameter settings. Batch size $BS = 32$. **Please note that this table is still being updated.**

References

- [1] Anastasios Arsenos, Dimitrios Kollias, and Stefanos Kollias, “A large imaging database and novel deep neural architecture for covid-19 diagnosis,” in 2022 IEEE 14th Image, Video, and Multidimensional Signal Processing Workshop (IVMSP). IEEE, 2022, p. 1–5.
- [2] Dimitrios Kollias, Anastasios Arsenos, and Stefanos Kollias, “Ai-mia: Covid-19 detection & severity analysis through medical imaging,” arXiv preprint arXiv:2206.04732, 2022.
- [3] Dimitrios Kollias, Anastasios Arsenos, Levon Soukissian, and Stefanos Kollias, “Mia-cov19d: Covid-19 detection through 3-d chest ct image analysis,” in Proceedings of the IEEE/CVF International Conference on Computer Vision, 2021, pp. 537–544.
- [4] Dimitrios Kollias, N Bouas, Y Vlaxos, V Brillakis, M Seferis, Ilianna Kollia, Levon Sukissian, James Wingate, and S Kollias, “Deep transparent prediction through latent representation analysis,” arXiv preprint arXiv:2009.07044, 2020.
- [5] Dimitris Kollias, Y Vlaxos, M Seferis, Ilianna Kollia, Levon Sukissian, James Wingate, and Stefanos D Kollias, “Transparent adaptation in deep medical image diagnosis.,” in TAILOR, 2020, p. 251–267.
- [6] Dimitrios Kollias, Athanasios Tagaris, Andreas Stafylopatis, Stefanos Kollias, and Georgios Tagaris, “Deep neural architectures for prediction in healthcare,” Complex & Intelligent Systems, vol. 4, no. 2, pp. 119–131, 2018.

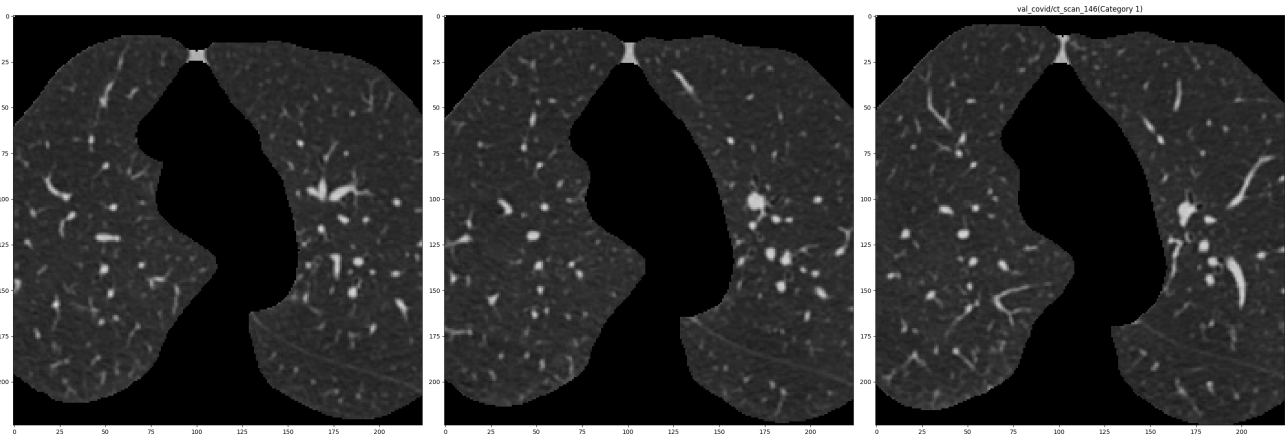


Figure 1: Example training input used to fine-tune CNNs.

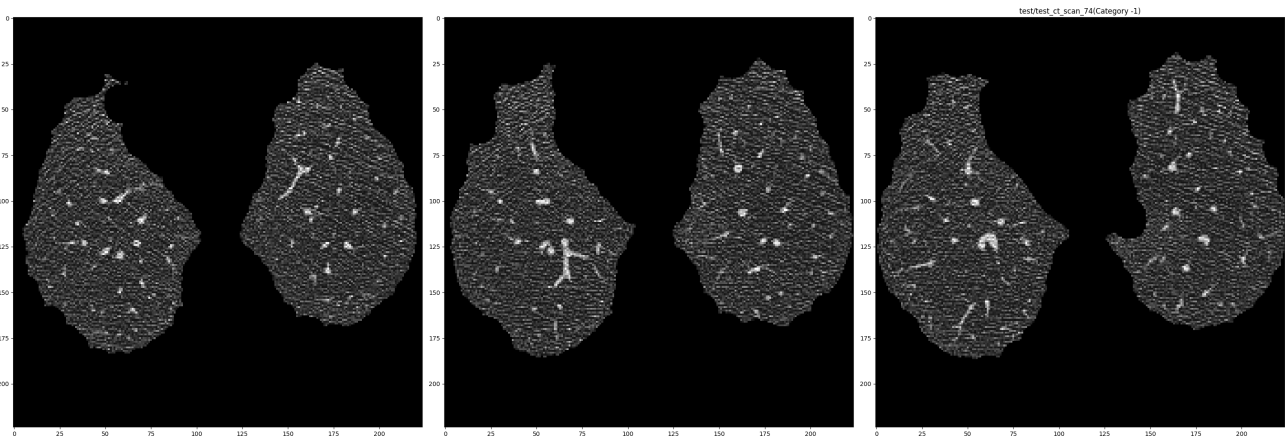


Figure 2: Example test input.

- [7] Saha M, Amin SB, Sharma A, Kumar TKS, Kalia RK. AI-driven quantification of ground glass opacities in lungs of COVID-19 patients using 3D computed tomography imaging. PLoS One. 2022;17(3):e0263916. Published 2022 Mar 14. doi:10.1371/journal.pone.0263916
- [8] Iandola, Forrest N., Song Han, Matthew W. Moskewicz, Khalid Ashraf, William J. Dally, and Kurt Keutzer. "SqueezeNet: AlexNet-level accuracy with 50x fewer parameters and 0.5 MB model size." arXiv preprint arXiv:1602.07360 (2016).
- [9] Szegedy, Christian, Vincent Vanhoucke, Sergey Ioffe, Jon Shlens, and Zbigniew Wojna. "Rethinking the inception architecture for computer vision." In Proceedings of the IEEE conference on computer vision and pattern recognition, pp. 2818-2826. 2016.
- [10] Zagoruyko, Sergey, and Nikos Komodakis. "Wide residual networks." arXiv preprint arXiv:1605.07146 (2016).
- [11] He, Kaiming, Xiangyu Zhang, Shaoqing Ren, and Jian Sun. "Deep residual learning for image recognition." In Proceedings of the IEEE conference on computer vision and pattern recognition, pp. 770-778. 2016.
- [12] Krizhevsky, Alex, Ilya Sutskever, and Geoffrey E. Hinton. "Imagenet classification with deep convolutional neural networks." Communications of the ACM 60, no. 6 (2017): 84-90.
- [13] Huang, Gao, Zhuang Liu, Laurens Van Der Maaten, and Kilian Q. Weinberger. "Densely connected convolutional networks." In Proceedings of the IEEE conference on computer vision and pattern recognition, pp. 4700-4708. 2017.
- [14] Dosovitskiy, Alexey, Lucas Beyer, Alexander Kolesnikov, Dirk Weissenborn, Xiaohua Zhai, Thomas Unterthiner, Mostafa Dehghani et al. "An image is worth 16x16 words: Transformers for image recognition at scale." arXiv preprint arXiv:2010.11929 (2020).
- [15] Simonyan, Karen, and Andrew Zisserman. "Very deep convolutional networks for large-scale image recognition." arXiv preprint arXiv:1409.1556 (2014).

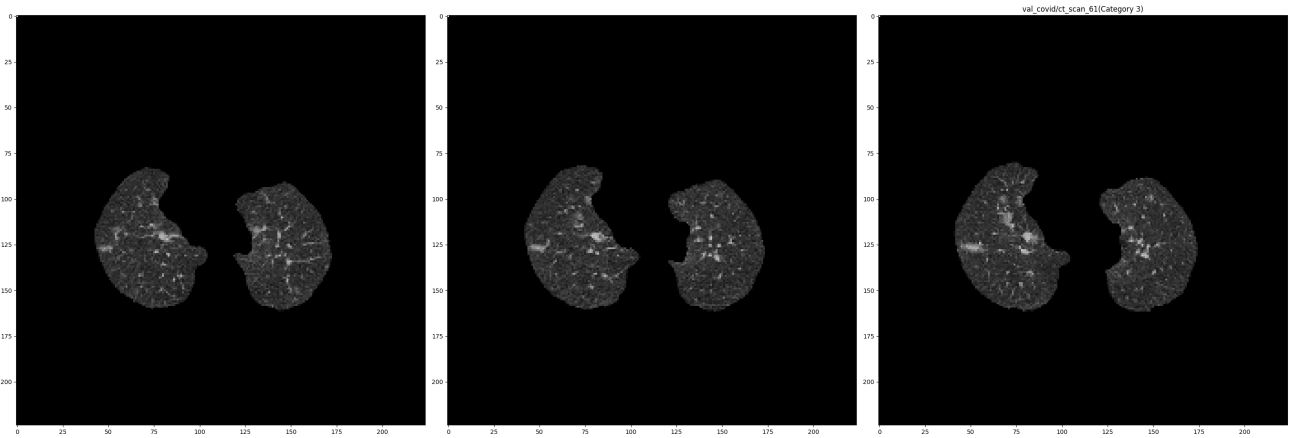


Figure 3: Another training input drawn from the severe class without application of the center-cropping.

- [16] Sergey P Morozov, Anna E Andreychenko, Ivan A Blokhin, Pavel B Gelezhe, Anna P Gonchar, Alexander E Nikolaev, Nikolay A Pavlov, Valeria Yu Chernina, and Victor A Gomboleviskiy, “MosMedData: data set of 1110 chest CT scans performed during the COVID-19 epidemic,” *Digital Diagnostics*, vol. 1, no. 1, pp. 49–59, 2020.
- [17] Lisa YW Tang, Harvey O Coxson, Stephen Lam, Jonathon Leipsic, Roger C Tam, and Don D Sin, “Towards large-scale case-finding: training and validation of residual networks for detection of chronic obstructive pulmonary disease using low-dose ct,” *The Lancet Digital Health*, vol. 2, no. 5, pp. e259–e267, 2020.
- [18] Huang, Gao, Zhuang Liu, Laurens Van Der Maaten, and Kilian Q. Weinberger. ”Densely connected convolutional networks.” In *Proceedings of the IEEE conference on computer vision and pattern recognition*, pp. 4700-4708. 2017.
- [19] Nagur Shareef Shaik and Teja Krishna Cherukuri, “Transfer learning based novel ensemble classifier for COVID-19 detection from chest ct-scans,” *Computers in Biology and Medicine*, vol. 141, pp. 105127, 2022.
- [20] Nathan Inkawhich, “Finetuning Torchvision Models,” https://pytorch.org/tutorials/beginner/finetuning_torchvision_models_tutorial.html, last modified 2017, accessed Mar 17, 2023.
- [21] Scott Mader “DST lung segmentation algorithm,” <https://www.kaggle.com/code/kmader/dsb-lung-segmentation-algorithm>, last modified 2017, accessed Mar 18, 2023.